Progress In Electromagnetics Research M, Vol. 94, 19–29, 2020

PBG Structured Compact Antenna with Switching Capability in Lower and Upper Bands of 5G

Jasmine Saini* and Manoj K. Garg

Abstract—A novel integrated compact antenna with photonic band gap (PBG) structure, having switching capability between lower and upper bands of 5G cellular communication is proposed. The proposed antenna can operate in the lower band (3.1 GHz to 3.5 GHz) as well as in the upper band (24 GHz to 27 GHz) of 5G cellular communication. Two radiating patches for the aforementioned frequency bands are developed in the same structure. A small patch for the upper-frequency band is inserted into a rectangular slot made in a large patch of the lower-frequency band. Both patches radiate at different times with the same ground. Two PIN diodes have been used to excite both patches at different times. The results indicate that the antenna has higher gain and wider bandwidth than the conventional antenna without a PBG structure.

1. INTRODUCTION

Wireless communication technology is evolving at a fast pace. 5G is a next-generation wireless communication technology, which provides support for very high speed data transfer. This technology would enable internet of things (IoT) and robotics applications to work effectively [1, 2]. With 5G, an integrated compact antenna is required that can transmit and receive the signal within the proposed lower and upper bands. Along with the conventional lower band, 5G technology also works in an upper band (millimeter wave) to achieve a larger bandwidth, higher data transfer rate, and low latency. Many researchers have proposed 5G microstrip antennas for lower and upper bands respectively [3–14]. Recently, photonic band gap (PBG) structures have attracted the attention of researchers in antenna design due to the property of lattice periodicity in space. It is because it can efficiently suppress the surface waves and higher order harmonics. The conventional microstrip antennas have the disadvantages of lower efficiency and narrow bandwidth due to the effect of surface waves [15, 16]. PBG structures provide stopbands, which eliminate the propagation of some frequencies, which affects radiation properties of antennas [17–28]. Zaidi et al. in [17] have designed a microstrip patch antenna at millimetre wave frequencies using a PBG cover and PBG substrate. They have reported gain improvement from 7.77 dB to 15.52 dB, but their reflection coefficient (S_{11}) has increased significantly from −31.24 dB to −17.26 dB. In [18], a design strategy using a PBG structure on ground plane is used to achieve wider bandwidth for patch antenna. The authors have reported an improvement in the impedance bandwidth from 3.72% to 31.9% at centre frequency 9 GHz after adding PBG on the ground plane. In [19, 20], the works reported also show enhancement in gain and bandwidth. The works attempted so far in the literature are either in the low-frequency band or in the upper frequency band. Recently, a new class of antennas using metamaterials has attracted the interest of many researchers. These artificial materials can enhance the characteristics of miniaturized antennas. A compact high gain rectangular dielectric resonator antenna using metamaterial as a superstrate for C-band applications is proposed in [29]. Authors have reported the increases in the peak gain of the antenna by 86%.

Received 22 February 2020, Accepted 23 June 2020, Scheduled 5 July 2020
* Corresponding author: Jasmine Saini (jasmine.saini@jiit.ac.in).
The authors are with the Department of Electronics and Communication Engineering, Jaypee Institute of Information Technology, A10, Sector-62, Noida, Uttar Pradesh 201307, India.

Electromagnetic band gap (EBG) antennas are also becoming a popular choice among researchers because of its ability to offer unique solutions for effectively manipulating EM waves over a broad range of frequencies.

In [30, 31], a split ring resonator (SRR) based EBG structure and hemispherical dielectric resonator antenna on an EBG substrate, respectively, are discussed for broadband and high gain systems. The works attempted so far in the literature are either in the low-frequency band or in the upper frequency band. In the proposed work, the antenna has been designed to work with the same structure in both bands of 5G technology.

2. ANTENNA DESIGN CONSIDERATION

The proposed antenna is designed and simulated on HFSS software. A Rogers 5880, having a dielectric constant of 2.2, loss tangent of 0.0013, and standard height of 1 mm, is taken as a dielectric material for substrate. Dimensions of the patch for the proposed antenna are calculated using the well-known microstrip patch antenna formulas as stated below [32].

The dimensions of the ground and substrate are the same ($L_g \times W_g$) which can be calculated by using the formula given in Equations (6) and (7), respectively. The selected dimensions of the radiating patch 1 ($L_{p1} \times W_{p1}$), patch 2 ($L_{p2} \times W_{p2}$), and ground are given in Table 1. The top view of the radiating patch, bottom views of ground with and without the PBG structure are shown in Figure 1. To obtain the desired bandwidth and gain, a 2D PBG structure is formed by cutting the sixteen square blocks of size ($a \times a$) at the ground plane as shown in Figure 1(c).

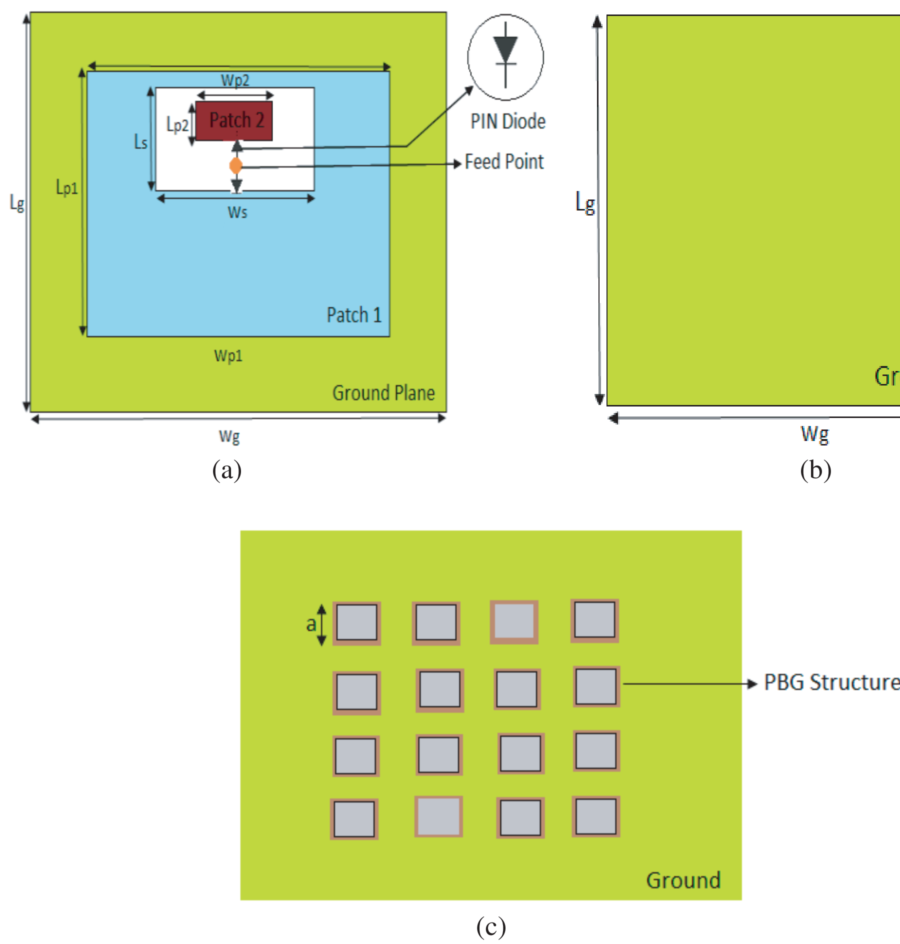

Figure 1. Geometry of the proposed antenna. (a) Top view. (b) Bottom view without PBG. (c) Bottom view with PBG.

Table 1. Design parameters of the antenna.

Dimensions	**Values (mm)**
L_{p1}	26
W_{p1}	30
L_{p2}	4.5
W_{p2}	8.5
L_s	8
W_s	12
L_g	44
W_g	48
A	5

Width of the patch

$$W = \frac{c}{2f_0\sqrt{\frac{(\varepsilon_r+1)}{2}}} \tag{1}$$

Effective dielectric constant

$$\varepsilon_{\mathit{eff}} = \frac{(\varepsilon_r+1)}{2} + \frac{(\varepsilon_r-1)}{2}\left[1+12\frac{h}{w}\right] \tag{2}$$

Effective length

$$\mathrm{L}_{\mathit{eff}} = \frac{c}{2f_0\sqrt{\varepsilon_{\mathit{eff}}}} \tag{3}$$

Length extension

$$\Delta L = 0.412h\frac{(\sqrt{\varepsilon_{\mathit{eff}}}+0.3)\left(\frac{W}{h}+0.264\right)}{(\sqrt{\varepsilon_{\mathit{eff}}}-0.258)\left(\frac{W}{h}+0.8\right)} \tag{4}$$

The actual length of the patch

$$L = L_{\mathit{eff}} - 2\Delta L \tag{5}$$

Length of Ground plane

$$L_g = L + 6h \tag{6}$$

Width of Ground plane

$$W_g = W + 6h \tag{7}$$

where the following parameters are used

f_0 is the resonant frequency;
W is the width of the patch;
L is the length of the patch;
h is the thickness of the substrate;
ε_r is the relative permittivity of the dielectric substrate;
c is the Speed of light: 3×10^8 m/s.

Both patches are designed according to the bands proposed by Telecom Regulatory Authority of India (TRAI) and their resonant frequencies. Dimensions of both bands (lower and upper) have been calculated according to their resonant frequencies 3.3 GHz and 25.5 GHz, respectively. Patch 2 is fixed inside the rectangular slot made in patch 1. But the slot cut in patch 1 itself generates the

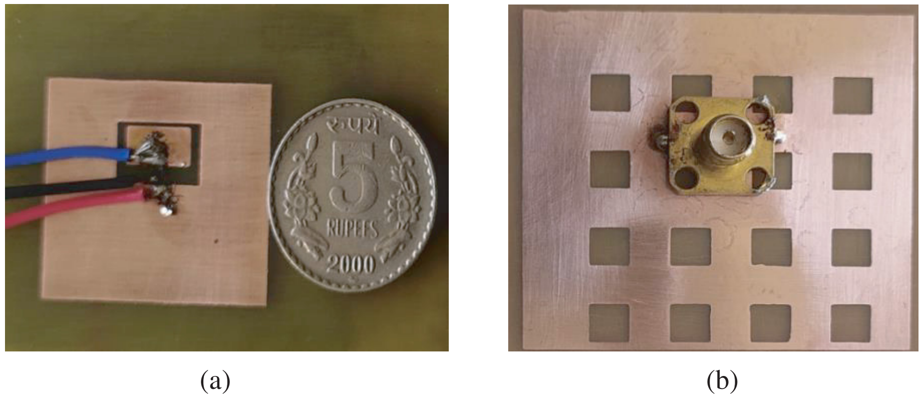

Figure 2. Fabricated antenna with PBG structure. (a) Top view. (b) Bottom view.

resonant frequency of a higher mode. The high frequency generated by the rectangular slot should not interfere in both the bands, thus, it is important to take this frequency between the two bands. The resonant frequencies of higher modes generated by rectangular slots created in patch 1 can be changed by changing the slots' dimensions [33, 34]. A PBG structure has been built on the ground plane to improve the desired bandwidth and other characteristics of the antenna. The top and bottom views of the fabricated antenna with PBG structured ground plane are presented in Figure 2. A periodic PBG structure is designed on the ground plane with the help of 16 small squares. A coaxial probe with 50-ohm characteristic impedance has been used to feed both the patches (Patch 1 and Patch 2) with the help of two PIN diodes.

Switching ON or OFF of these two PIN diodes is controlled by an external biasing circuit with the help of a microcontroller as shown in Figure 3. This biasing circuit consists of two blocking capacitors of value 0.1 μF each and two inductor coils of value 6.8 nH each. Two blocking capacitors (C_{b1} and C_{b2}) help to protect the antenna from the DC voltage.

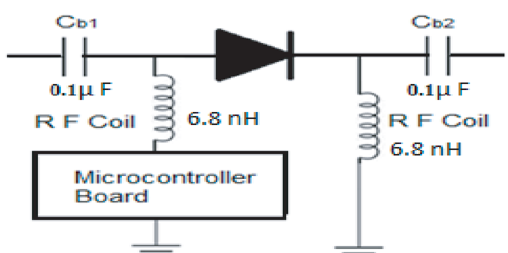

Figure 3. Biasing circuit using microcontroller board.

3. RESULTS AND DISCUSSIONS

The patches can be connected with the coaxial feed probe by turning PIN diode 1 and PIN diode 2 in ON or OFF state.

When PIN 1 turns on, patch 1 is excited and radiates in the lower band of 5G with resonant frequency 3.14 GHz and the reflection coefficient of −25.8 dB as shown in Figure 4(a). Similarly, on the excitation of patch 2, the antenna radiates in the upper band of 5G with resonant frequency 24.63 GHz and reflection coefficient of −32.54 dB as shown in Figure 4(b).

From Figure 4, it can be observed that the bandwidths of the lower and upper bands (without PBG structure) are 50 MHz and 1420 MHz, respectively, which are insufficient for 5G applications. For bandwidth enhancement, a 2D PBG structure is etched on the ground plane. This periodic pattern of sixteen square blocks is shown in Figure 1(c).

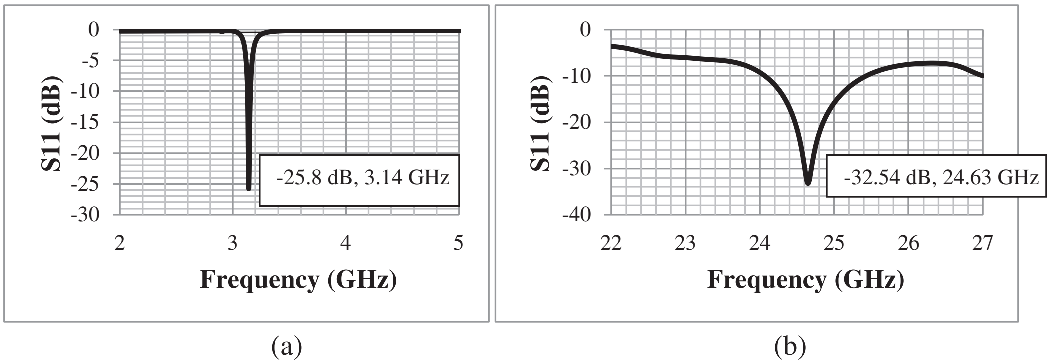

Figure 4. Return loss of the antenna without PBG structure. (a) Lower band. (b) Upper band.

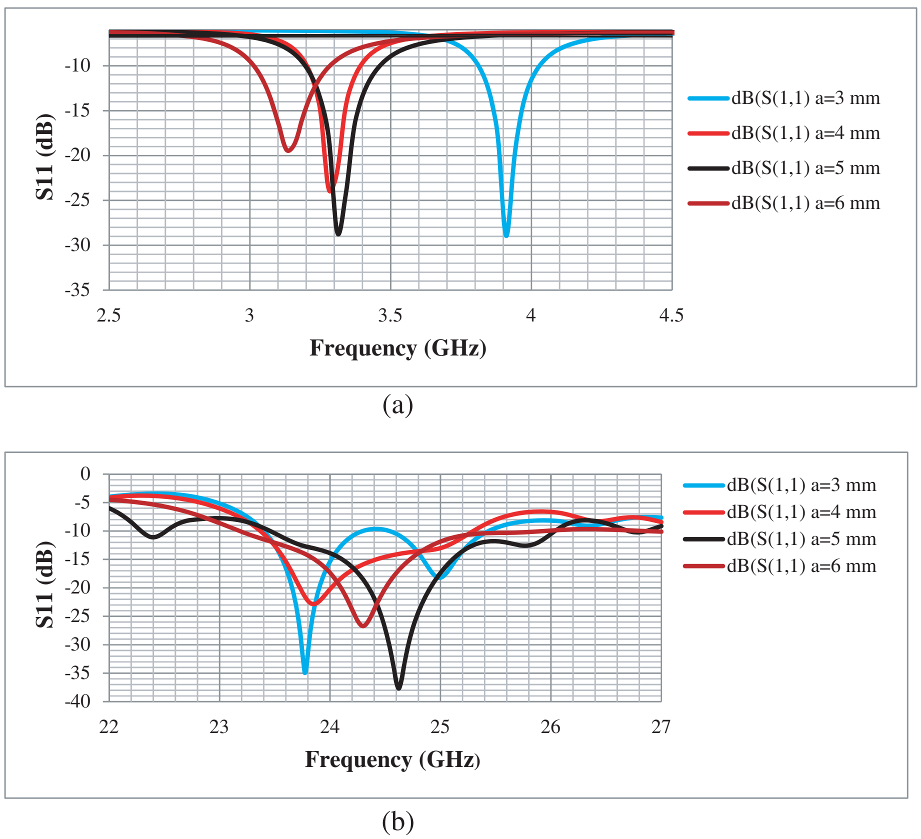

Figure 5. Return loss at different PBG dimensions for (a) lower band, (b) upper band.

The dimensions of square blocks are optimized for wider bandwidth using optometric analysis. Return loss simulations are carried out for different dimensional values of side 'a' ($a = 3, 4, 5$ and $6\,\text{mm}$) of the square block as shown in Figures 5(a) and 5(b).

It is clearly evident that with increasing the size of the square block made in the PBG structure, the bandwidth of both bands also increases. The return loss and corresponding bandwidth at different values of square slot dimensions are tabulated in Table 2. It is evident from the optometric analysis of both the bands that keeping $a = 5\,\text{mm}$, best results can be obtained. The PBG structure not only increases the bandwidth of the antenna but also improves its gain and directivity. The gains of the antenna (simulated and measured) at the lower and upper bands without and with PBG structure are

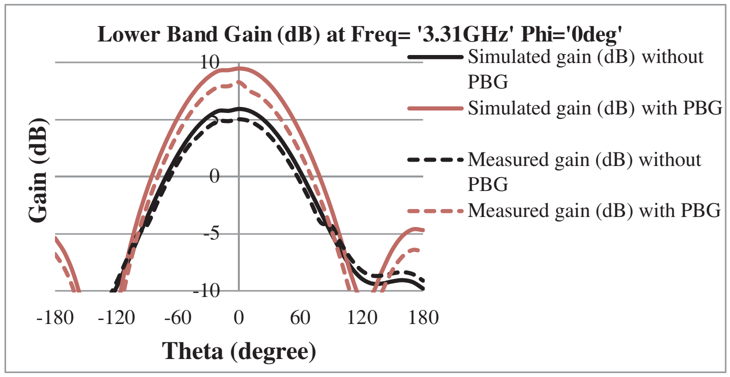

(a)

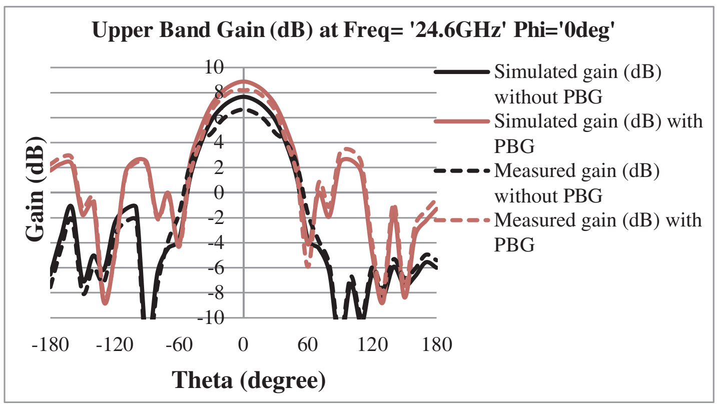

(b)

Figure 6. Measured and simulated antenna gain without and with PBG structure of (a) lower band, (b) upper band.

shown in Figure 6. In the upper band, the gain pattern is not very smooth as evident from Figure 6(b). Due to the cutting of slots, side lobe and back lobe levels are increased slightly at the upper band. This is because the size of the PBG structure becomes comparable to the wavelength at higher frequencies. At the same time, the bandwidth is increased many folds in upper band due to cutting the PBG structure on the ground plane. So, there is a tradeoff with the side lobe and back lobe radiation to some extent to get wider bandwidth in the upper band of 5G. The measured and simulated return losses with the PBG structure of the lower and upper bands of 5G are shown in Figure 7. All results (return loss, gain, and bandwidth) of the lower and upper bands without and with PBG structure are tabulated in Table 3. By using PBG structure, gain, bandwidth, and reflection coefficient are improved by 3.54 dB, 530 MHz, and −3.2 dB in the lower band and 1.2 dB, 1200 MHz, and −5.36 dB in the upper band respectively.

Table 2. Results of optometric analysis.

	Lower Band			Upper Band		
a (mm)	S_{11} (dB)	Range (GHz)	BW (MHz)	S_{11} (dB)	Range (GHz)	BW (MHz)
3	−28	3.79–4.03	240	−34.7	23.4–24.2	800
4	−23	3.19–3.44	250	−22.7	23.3–25.2	1900
5	−28.5	3.19–3.46	270	−37.6	23.49–25.96	2470
6	−19.3	3.01–3.30	290	−26.7	23.12–25.9	2780

Table 3. Comparison of parameters (without PBG structure and with PBG structure).

Bands	Type of Ground	Simulated Results			Measured Results		
		S_{11} (dB)	Gain (dB)	Bandwidth (MHz)	S_{11} (dB)	Gain (dB)	Bandwidth (MHz)
Lower Band	Without PBG Structure	−25.8	5.92	50 (3.1–3.15 GHz)	−24	5.02	49 (3.21–3.259 GHz)
	With PBG Structure	−29	9.46	580 (3.13–3.71 GHz)	−25.20	8.26	580 (3.34–3.92 GHz)
Upper Band	Without PBG Structure	−32.5	7.66	1420 (24.16–25.58 GHz)	−30.90	6.64	1410 (25.51–24.10 GHz)
	With PBG Structure	−38	8.8	2620 (23.4–26.02 GHz)	−31.80	8.18	2600 (23.5–26.1 GHz)

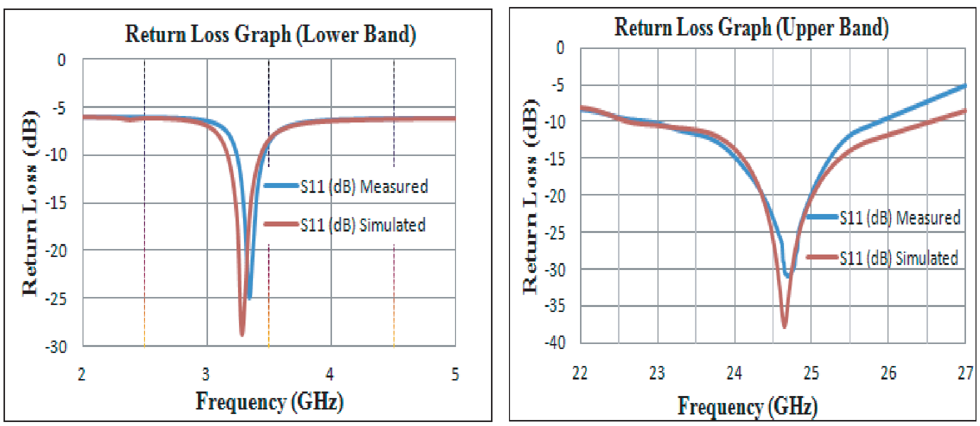

(a) (b)

Figure 7. Simulated and measured return loss with PBG structure. (a) Lower band. (b) Upper band.

The surface current distributions of patch 1 and patch 2 are shown in Figure 8. When patch 1 is excited, the surface current density can be observed everywhere on patch 1, and negligible current lies on patch 2 due to the mutual induction between patch 1 and patch 2. It shows that the mutual induction between patch 1 and patch 2 is negligibly small, i.e., the performance of patch 1 will not be deteriorated due to the presence of patch 2. On the other hand, when we excite patch 2, the surface current density can be observed everywhere on patch 2, and a significant but very small current lies on patch 1 due to the mutual induction between patch 1 and patch 2. From Figure 8(b), it is clear that the current on patch 1 due to induction ends within very small distance, i.e., the performance of patch 2 will not be deteriorated significantly. Cross-polarization is the orthogonal polarization, and it should be as low as possible. A simple way of minimizing such effects is by using a defective ground plane [35]. The number of squares cut on the ground plane is optimized to reduce this effect. Measurement of cross polarization is calculated as the ratio of maximum gain of cross-polarization to maximum gain of co-polarization. The cross-polarization and co-polarization effects at the lower and upper frequency bands for the two values of the angle φ (0° and 90°) are shown in Figures 9 and 10, respectively. Table 4 gives the values of cross polarization at different values of φ.

After observing the results, it can be seen that there is a substantial improvement in the antenna characteristics like gain, return loss, bandwidth after employing PBG structure. From Table 3, it can be observed that the simulated and measured results are in good agreement.

(a) (b)

Figure 8. Surface current distribution when (a) patch 1 is excited (b), patch 2 is excited.

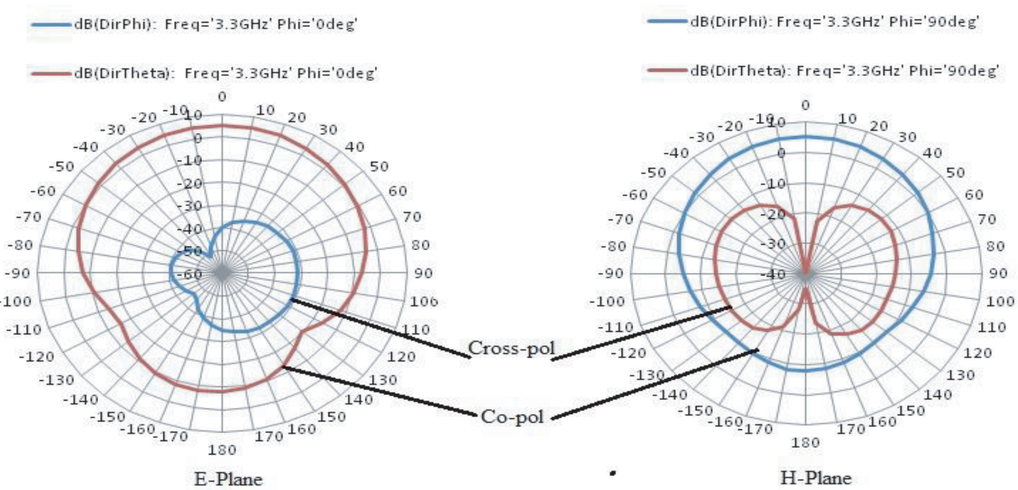

(a) (b)

Figure 9. Cross polarization effect at lower frequency band (a) $\phi = 0°$. (b) $\phi = 90°$.

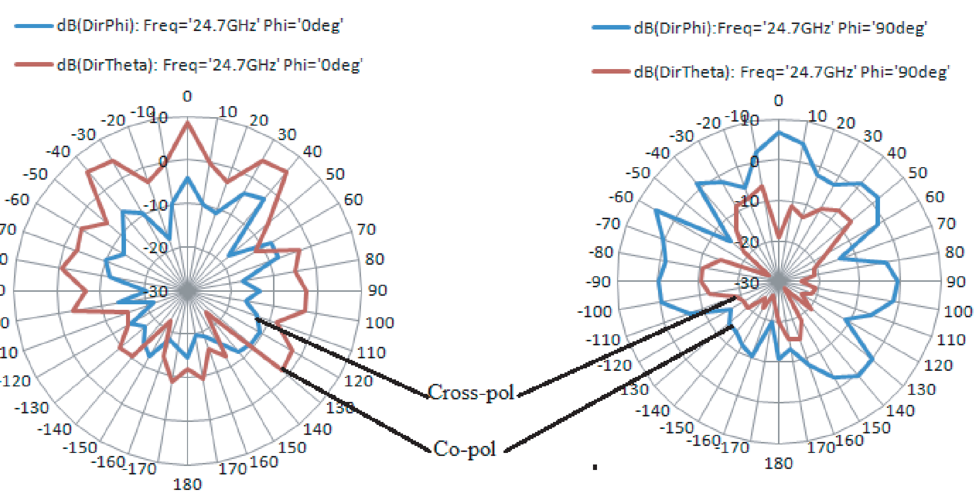

(a) (b)

Figure 10. Cross polarization effect at upper frequency band (a) $\phi = 0°$. (b) $\phi = 90°$.

Table 4. Cross polarization values in lower and upper bands.

S. No	Angle φ	Cross polarization in dB	
		Lower frequency band	Upper frequency band
1	$\varphi = 0°$	-37.05	-11.09
2	$\varphi = 90°$	-20.41	-13.11

4. CONCLUSION

The proposed antenna provides the flexibility to work in either a low-frequency band or an upper frequency band of 5G. Both bands can be switched alternately by electronic methods. Besides, this novel antenna based on a PBG structure has enhanced the characteristics of antenna like gain, bandwidth, etc. manifold. From the simulated and measured results, it is observed that the antenna's gain, bandwidth, and return loss are significantly improved by using a PBG structure. Therefore, PBG structures are helpful in enhancing the characteristics of antennas, thus making them suitable for future 5G and high frequency applications.

REFERENCES

1. See, C. H., R. A. Abd-Alhameed, A. A. Atojoko, N. J. McEwan, and P. S. Excell, "Link budget maximization for a mobile band subsurface wireless sensor in challenging water utility environments," *IEEE Transactions on Industrial Electronics*, Vol. 65, No. 1, 616–625, Jan. 2018.
2. *A White Paper on Enabling 5G in India*, Telecom Regulatory Authority of India, Feb. 22, 2019.
3. Hong, W., Z. H. Jiang, C. Yu, J. Zhou, P. Chen, and Z. Yu, "Multibeam antenna technologies for 5G wireless communications," *IEEE Transactions on Antennas and Propagation*, Vol. 65, No. 12, 6231–6249, Dec. 2017.
4. Ashraf, N., O. Haraz, M. A. Ashraf, and S. Alshebeili, "28/38-GHz dual-band millimeter-wave SIW array antenna with EBG structures for 5G applications," *2015 International Conference on Information and Communication Technology Research (ICTRC)*, 5–8, 2015.
5. Cheng, H. R., Q. Song, Y.-C. Guo, X.-Q. Chen, and X.-W. Shi, "Design of a novel EBG structure and its application in fractal microstrip antenna," *Progress In Electromagnetics Research C*, Vol. 11, 81–90, 2009.
6. An, W., Y. Li, H. Fu, J. Ma, W. Chen, and B. Feng, "Low-profile and wideband microstrip antenna with stable gain for 5G wireless applications," *IEEE Antennas and Wireless Propagation Letters*, Vol. 17, No. 4, 621–624, Apr. 2018.
7. Aliakbari, H., A. Abdipour, R. Mirzavand, A. Costanzo, and P. Mousavi, "A single feed dual-band circularly polarized millimeter-wave antenna for 5G communication," *2016 10th European Conference on Antennas and Propagation (EuCAP)*, 1–5, 2016.
8. Firdausi, A., G. Hakim, and M. Alaydrus, "Designing a tri-band microstrip antenna for targetting 5G broadband communications," *MATEC Web of Conferences*, Vol. 218, 03015, ICIEE, 2018.
9. Mak, K. M., H. W. Lai, K. M. Luk, and C. H. Chan, "Circularly polarized patch antenna for future 5G mobile phones," *IEEE Access*, Vol. 2, 1521–1529, Dec. 2014.
10. Neto, A. S. E. S., M. L. M. Dantas, J. S. Silva, and H. C. C. Fernandes, "Antenna for the fifth-generation (5G) using an EBG structure," *Advances in Intelligent Systems and Computing*, Vol. 354, 33–38, Springer International Publishing Switzerland 2015, 2015.
11. Haraz, O., M. M. M. Ali, A. Elboushi, and A. Sebak, "Four-element dual-band printed slot antenna array for the future 5G mobile communication networks," *2015 IEEE International Symposium on Antennas and Propagation & USNC/URSI National Radio Science Meeting*, 1–2, Jul. 2015.

12. Haraz, O. M., A. Elboushi, S. A. Alshebeili, and A. R. Sebak, "Dense dielectric patch array antenna with improved radiation characteristics using EBG ground structure and dielectric superstrate for future 5G cellular networks," *IEEE Access*, Vol. 2, 909–913, 2014.
13. Chu, C., J. Zhu, S. Liao, A. Zhu, and Q. Xue, "28/38 GHz dual-band dual-polarized highly isolated antenna for 5G phased array applications," *2019 IEEE MTT-S International Wireless Symposium (IWS)*, 1–3, Guangzhou, China, May 19–22, 2019.
14. Saedi, H. A., J. A. Attari, W. M. A. Wahab, R. Mittra, and S. S. Naeini, "Single-feed dual-band aperture-coupled antenna for 5G applications," *18th International Symposium on Antenna Technology and Applied Electromagnetics (ANTEM)*, Aug. 19–22, 2018.
15. Singh, P. K. and J. Saini, "Effect of varying curvature and inter element spacing on dielectric coated conformal microstrip antenna array," *Progress In Electromagnetics Research M*, Vol. 58, 11–19, 2017.
16. Singh, P. K. and J. Saini, "Reconfigurable microstrip antennas conformal to cylindrical surface," *Progress In Electromagnetics Research Letters*, Vol. 72, 119–126, 2018.
17. Zaidi, A., A. Baghdad, A. Ballouk, and A. Badri, "High gain microstrip patch antenna, with PBG substrate and PBG cover, for millimeter wave applications," *2018 4th International Conference on Optimization and Applications (ICOA)*, 1–6, Mohammedia, 2018.
18. AbuTarboush, H. F., H. S. Al-Raweshidy, and R. Nilavalan, "Bandwidth enhancement for small patch antenna using PBG structure for different wireless applications," *2009 IEEE International Workshop on Antenna Technology*, 1–4, Santa Monica, CA, 2009.
19. Qian, Y., R. Coccioli, D. Sievenpiper, V. Radisic, and E. Yablonovitch, "A microstrip patch antenna using novel photonic band-gap structures," *Microwave Journal*, Vol. 42, 66–71, Jan. 1999.
20. Wu, Y. and T. Fu, "The study on a patch antenna with PBG structure," *2009 Third International Symposium on Intelligent Information Technology Application*, 565–567, Shanghai, 2009.
21. Jha, K. R. and G. Singh, "Analysis and design of terahertz microstrip antenna on photonic bandgap material," *Journal of Computation Electronics*, Vol. 11, No. 4, 364–373, 2012.
22. Temelkuran, B., M. Bayindir, E. Ozbay, R. Biswas, M. M. Sigalas, G. Tuttle, and K. M. Ho, "Photonic crystal-based resonant antenna with very high directivity," *Journal of Applied Physics*, Vol. 87, No. 1, 603–605, Jan. 2000.
23. Singh, A. and S. Singh, "A trapezoidal microstrip patch antenna on photonic crystal substrate for high speed THz applications," *Photonics Nanostructures Fundamentals Applied*, Vol. 14, 52–62, 2015.
24. Kushwaha, R. K., P. Karuppanan, and L. D. Malviya, "Design and analysis of novel microstrip patch antenna on photonic crystal in THz," *Physica B Condensed Matter*, Vol. 545, 107–112, 2018.
25. Nejati, A., R. A. Sadeghzadeh, and F. Geran, "Effect of photonic crystal and frequency selective surface implementation on gain enhancement in the microstrip patch antenna at terahertz frequency," *Physica B Condensed Matter*, Vol. 449, 113–120, 2014.
26. Dadras, M., P. Rezaei, and M. Danaie, "Planar double-band monopole antenna with photonic crystal structure," *Indian J. Sci. Technology*, Vol. 8, No. 36, 1–4, 2016.
27. Wu, Y. and T. Fu, "The study on a patch antenna with PBG structure," *2007 Workshop on Intelligent Information Technology Applications*, Vol. 3, 565–567, Nov. 21–22, 2009.
28. AbuTarboush, H. F., H. S. Al-Raweshidy, and R. Nilavalan, "Bandwidth enhancement for patch antenna using PBG slot structure for 5, 6 and 9 GHz applications," *2009 IEEE 10th Annual Wireless and Microwave Technology Conference*, 1–1, Apr. 20–21, 2009.
29. Pandey, A. K., M. Chauhan, V. Killamsetty, and B. Mukherjee, "High gain compact rectangular dielectric resonator antenna using metamaterial as superstrate," *International Journal of RF and Microwave Computer-Aided Engineering*, Vol. 29, No. 12, 1–10, Wiley, 2019.
30. Sinha, M., V. Killamsetty, and B. Mukherjee, "Near field analysis of rdra loaded with split ring resonators superstrate," *Microwave and Optical Technology Letters*, Vol. 60, No. 2, 472–478, Wiley, 2018.

31. Mukherjee, B., D. Kumar, and M. Gupta, "A novel hemispherical dielectric resonator antenna on an electromagnetic band gap substrate for broadband and high gain systems," *AEU – International Journal of Electronics and Communication*, Vol. 68, 1185–1190, Elsevier, 2014.
32. Liu, S., S. Qi, W. Wu, and D. Fang, "Single-layer single-patch four-band asymmetrical U-slot patch antenna," *IEEE Transactions on Antennas and Propagation*, Vol. 62, No. 9, 4895–4899, Sept. 2014.
33. Garg, M. K. and J. Saini, "Multi-band and multi-parameter reconfigurable slotted patch antenna with embedded biasing network," *(IJACSA) International Journal of Advanced Computer Science and Applications*, Vol. 10, No. 10, 2019.
34. Hocinia, A., M. N. Temmara, D. Khedrouchea, and M. Zamanib, "Novel approach for the design and analysis of a terahertz microstrip patch antenna based on photonic crystals," *Photonics and Nanostructures — Fundamentals and Applications*, Vol. 36, 100723, Sept. 2019.
35. Kumar, C., M. I. Pasha, and D. Guha, "Microstrip patch with non-proximal symmetric defected ground structure(DGS) for improved cross-polarization properties over principal radiation planes," *IEEE Antennas and Wireless Propagation Letters*, Vol. 14, 1412–1414, Feb. 2015.